

Distinguishing Till Members in Minnesota Using Trace and Rare Earth Elements

By

Russell Krueger

A thesis submitted in partial fulfillment of the requirements of the degree of

Bachelor of Arts
(Geology)

at

Gustavus Adolphus College

2017

Distinguishing Till Members in Minnesota Using Trace and Rare Earth Elements
By
Russell Krueger
Under the supervision of Dr. Julie Bartley

ABSTRACT

Glacial sediments preserve a record of their source area, as glaciers erode the bedrock and deposit the eroded material as till. Typically, provenance is determined through interpretations of physical characteristics, but this method can be inconsistent because of biases among observers. Geochemical fingerprinting might distinguish between two visibly similar till members, but this is a relatively new technique and a universal method has not yet been developed. Most notably, different sediment size fractions have been used in geochemical studies; some use < 2 mm, while others use < 63 μm . To move toward a universal method, trace and rare earth element concentrations were analyzed for four till members of known provenance from a single core in Renville County, MN. Each sample was sieved to obtain both size fractions, and the same analysis was performed for each size. Discriminant functional analysis was used to distinguish between the till groups, and the classification accuracy for each size fraction exceeded 80% (< 2 mm : 86.9%; < 63 μm : 82.6%). Seven elements were influential in distinguishing members using the < 2 mm fraction (V, Cu, Rb, Ho, Tm, Pb, U), while 10 elements were required for < 63 μm (V, Cr, Cu, Rb, Y, Eu, Pr, Tm, Pb, U). The results indicate that sieving to and analyzing the < 2 mm size fraction is acceptable for determining till provenance.

ACKNOWLEDGEMENTS

I would like to thank Sigma Xi for providing the funding for lab materials. I would also like to thank the Minnesota Geological Survey (MGS) for providing samples. Thank you to Dr. Laura Triplett, Dr. Julie Bartley, and Dr. Andrew Haveles for their guidance in the development, analysis, and writing process. Without their tutelage, the project would not be half of what it turned out to be. Dr. Bartley also assisted in communicating with MGS to set up the project. Thank you to Dr. Jeff Jeremiason for the use of his lab's ICP-MS, this project's main instrument. I would also like to thank the Gustavus Adolphus College Geology department for the use of their lab space and furnace. Finally, thank you to Tanner Eischen and Ruby Schaffler for their assistance in completing all of the fusions.

TABLE OF CONTENTS

Abstract	pg 2
Introduction	pg 5
Geologic Setting	pg 8
Methods	pg 11
Results	pg 13
Discussion	pg 25
Conclusion	pg 29
References	pg 29
Appendix A: Quality Assurance and Quality Control	pg 31
Appendix B: Standards used	pg 32
Calibration standards	
Green River Shale (SGR-1)	
Post-Archean Australian Shale (PAAS)	

Figures and Tables

<u>Figure/Table</u>	<u>Title</u>	<u>Page number</u>
Figure 1	Map of Wisconsin Age glacial movement	9
Figure 2	Location of Renville County within Minnesota	9
Figure 3	Simplified stratigraphy of core RNR-2	10
Figure 4	Trace element trend with depth	14
Figure 5	Spider diagrams of different size fractions	15
Table 1	ANOVA results for both size fractions	16
Figure 6	PCA results for all and REE-only <2 mm	17
Figure 7	PCA results for all and REE-only <63 μ m	17
Table 2	Preliminary DFA scaling factors	19
Figure 8	PCA of elements in final DFA model <2 mm	20
Figure 9	Results of final DFA model <2 mm	20
Figure 10	PCA of elements in final DFA model <63 μ m	21
Figure 11	Results of final DFA model <63 μ m	22
Table 3	Cross-validation table for <2 mm DFA model	23
Table 4	Cross-validation table for <63 μ m DFA model	23
Figure 12	Villard overlain on final DFA models for both sizes	24

INTRODUCTION

Most areas of Minnesota are covered by glacial till as glaciers advanced and retreated across the landscape over the last two million years. These tills impact their surrounding environments. Elements in till can leach into groundwater below or be taken up by plants in the soil above. For example, studies have noted that arsenic and sulfate in ground water can be traced to certain tills (Erickson 2005; Grasby 2010). High arsenic levels have been discovered in groundwater wells in Des Moines Lobe till in Minnesota (Erickson 2005). Others have noted that traces of economic resources can travel large distances through till, and knowing the provenance of resource rich tills helps in resource exploration (Shilts 1995; Ohlander 1996). Methods that – rapidly and in small sample sizes – permit till units to be distinguished are highly sought after by geological surveys. Geochemical fingerprinting – the process of discerning multi-element patterns of concentration within a sample – is a promising method to quickly distinguish among till members.

Till members (or units) are distinct, stratigraphic layers that were deposited during glacial advance and retreat, and are often identified by differences in lithology associated with provenance, the sediment's original location. Repeated cycles of glacial advance and retreat can cause units of different provenance to accumulate in one location. To assess sequences containing many units, glacial tills are sampled using a sediment core to obtain a succession of material. Sediment samples are taken along the length of the core at defined intervals. The most common way to determine provenance is through the clast-count method. In this method, the proportion of shale, carbonate, and crystalline material is determined; the mineralogy of the samples is also determined, typically through microscopy (Hobbs 1998). These characteristics are then compared to the bedrock geology of possible source areas to determine provenance. This method works because glaciers erode the bedrock of their source areas and deposit this material in the till, so the till retains the lithology of the source area.

Ultimately, the lithology controls the chemical nature of the till, so geochemical fingerprinting can provide an additional tool to determine provenance (Ohlander 1996; McMartin 2016). In order to collect geochemical information on bulk sediment, the sample must be homogenized and dissolved; one method is a fusion technique. Fusions involve melting a powdered sediment sample to produce a glass, ensuring the sample is homogenous. The glass is

dissolved in acid, which allows one to measure elemental concentrations using mass spectroscopy.

Within the provenance literature, one of two size fractions of the till are used: <2 mm (Gore 2003; Dempster 2013) or <63 μm (Farmer 2006; Thorleifson 2007). The rationale for each size depends on how a “characteristic sample” is defined. Those who use the <2 mm fraction say that this fraction contains is more representative of the sample, while those using <63 μm argue that the grains between 2 mm and 63 μm are primarily quartz and feldspars. These minerals are considered chemically homogeneous and therefore dilute the geochemical signature contained in the <63 μm fraction. A fusion method, coupled with multivariate statistical analysis was investigated to determine its applicability in distinguishing between four till members based on trace and rare earth element (REE) concentrations within a single stratigraphic core in Minnesota. The fusion preparation and multivariate statistical analysis were completed for each of the size fractions to investigate these influences.

PREVIOUS WORK

Provenance studies in Minnesota have largely relied on analysis of the larger than 2 mm grain (pebble) size fraction of the till. Current provenance determinations rely on pebble clast counts, which consider grain size, matrix carbonate content, and magnetic property analyses (Hobbs 1998; Gowan 1998). While these analyses require only minimal sample preparation, some problems arise when they are used alone. For example, the distinction between northwest and northeast provenance is largely based on the presence of limestone, but almost all northern Minnesota tills contain some carbonate (Gowan 1998). In addition, grain size and magnetic property analyses show considerable overlap between tills of different known provenance (Gowan 1998). The clast count method is reliant on interpretation, and these can differ by individual analyst. This method is usually adequate for determining the provenance area of till units, but discerning visually similar tills is often disputed (Knaeble, personal communication). Another method must be added to be able to definitively determine provenance of tills in Minnesota.

Other studies have implemented geochemical fingerprinting of tills for multiple purposes. A team in Finland successfully interpreted a till sequence collected from northern Finland through comparison of major element concentrations of the layers (Lunkka 2013). Another team

in Canada identified high sulfate groundwater concentrations were more prominent in groundwater below tills associated with the Laurentide Ice Sheet than those associated with the Cordilleran Ice Sheet (Grasby 2010). A team in Minnesota found a correlation between high arsenic levels in groundwater wells and wells drilled under Des Moines Lobe deposits (Erickson 2005). These studies did not directly measure the geochemistry of till, but they provide insight into how tills of different provenance can impact the surrounding environment. Knowing the geochemical signature of till can provide insight into potential environmental problems that could arise because of the till.

Gowan (1998) collected samples of surficial and sub-surficial tills of known provenance and conducted a 34-element geochemical analysis using Inductively Coupled Plasma Atomic Emission Spectroscopy. She found that each till is geochemically distinct, so that northeast and northwest provenance can be determined according to geochemistry (Gowan 1998). She noted that tills of similar provenance, but not necessarily the same glacial lobe are geochemically similar, but other tests could be used to aid in the determination (Gowan 1998). Additional studies have found that trace element concentrations increase in the silt and clay fractions, especially in clays with high phyllosilicate content (Shilts 1995; Klassen 1998). The use of the silt and clay fractions (<63 μm) fraction in geochemical analysis is thought to provide the best definition among tills, as the concentration ranges should be spaced farther apart. The use of the smaller size fraction should also allow for mapping at depth using drill cores. The silt and clay fractions are assumed to provide a better overall geochemical signature with less local influence (Shilts 1995; Gowan 1998). It should be noted that the silt and clay fraction are still affected by geochemical differences due to grain size and mineralogy. As mentioned earlier, trace element concentrations increase as grain size decreases (Shilts 1995). This phenomenon has been explained using mineralogy, as phyllosilicates generally have smaller terminal modes than other classes and have a structure that readily accepts trace element cations (Shilts 1995; Klassen 2001). Minerals that are more resistant to weathering and do not have a structure that accepts trace elements dilute the geochemical signature at larger grain sizes.

The use of REE concentrations in till provenance is not well-explored in the literature. Some studies have investigated the loss of REEs through weathering processes. REEs are generally considered immobile elements and thus can be very informative in geochemical studies (Ohlander 1996), particularly those related to provenance. A group from Sweden found that

REEs, especially the lighter ones, can be lost through weathering in both warm and cold climates (Ohlander 1996). This REE loss pattern may occur because minerals most commonly associated with elevated REE concentrations are often the most rapidly weathered. These minerals include amphibole, epidote, apatite, and plagioclase (Ohlander 1996).

Studies using trace element and REE concentrations to determine provenance use principal component analysis (PCA) to visualize the differences between groups (Dempster 2013; McMartin 2016). PCA is an exploratory multivariate statistical analysis in which each element is given a weighting factor to best represent the total variance between samples. In this manner, groups should be separated if different relationships between elements exist for each group. However, there is another multivariate statistics analysis that is designed to maximize the differences between each group and theoretically predict which group an unknown belongs to. This is called a discriminant function analysis, and was used in this investigation to determine the differences between the Minnesota till members.

GEOLOGIC SETTING

During the Pleistocene, Minnesota was almost entirely covered by glaciers. Only the southeast and southwest corners of the state remained ice-free (Lively 2009). The Laurentide Ice Sheet covered much of North America during the Pleistocene, with Minnesota located near its southern edge (Lively 2009). Four major ice advances occurred during the most recent glacial interval, the Wisconsin Age, which began about 75,000 years ago. The first two glacial lobes were active in the early to middle Wisconsin Age. The Rainy Lobe advanced from the northeast and reached east-central Minnesota (Gowan 1998). Its deposits are brown, sandy tills containing clasts of basalt and gabbro, which are typical of a northeast provenance. The exact provenance of the Wadena Lobe is disputed, as some state that it is a sublobe of the Rainy Lobe (Lively 2009) and others that it is a separate lobe with a more northwestern provenance (Gowan 1998; Thorleifson 2007). Its deposits are typically gray in color and contain limestone from the Winnipeg provenance (Figure 1). The observation that deposits of the Wadena Lobe are lithologically distinct suggest that it should be considered a separate lobe from the Rainy Lobe; it shall be considered as such in this thesis.

By the Late Wisconsin Age a third lobe, the Superior Lobe, advanced into Minnesota. This lobe also came from the northeast, specifically the Superior Basin. Its deposits are redder in color and contain sandstones, shales, and agates (Gowan 1998). This lobe reached the furthest south of the three (Figure 1). It may overlay Rainy Lobe deposits in some areas. The fourth and most recent lobe of the Wisconsin Age was the Des Moines Lobe. 14,000 years ago, this lobe advanced from the northwest through Minnesota and reached Des Moines, Iowa (Erickson 2005). During advance through Minnesota, this lobe split into two sublobes. The St. Louis sublobe travelled through the northern portion of Minnesota, and the Grantsburg sublobe travelled eastward, in the east-central part of the study (Figure 1). Des Moines Lobe deposits are gray to brown and contain Cretaceous shale from North Dakota and Canada (Lively 2009). Glaciers can also come from areas in between the general provenance areas or erode previously deposited till; till deposited under these circumstances contains material from multiple provenances. By 11,000 years ago, the glaciers retreated northward out of Minnesota (Lively 2009).

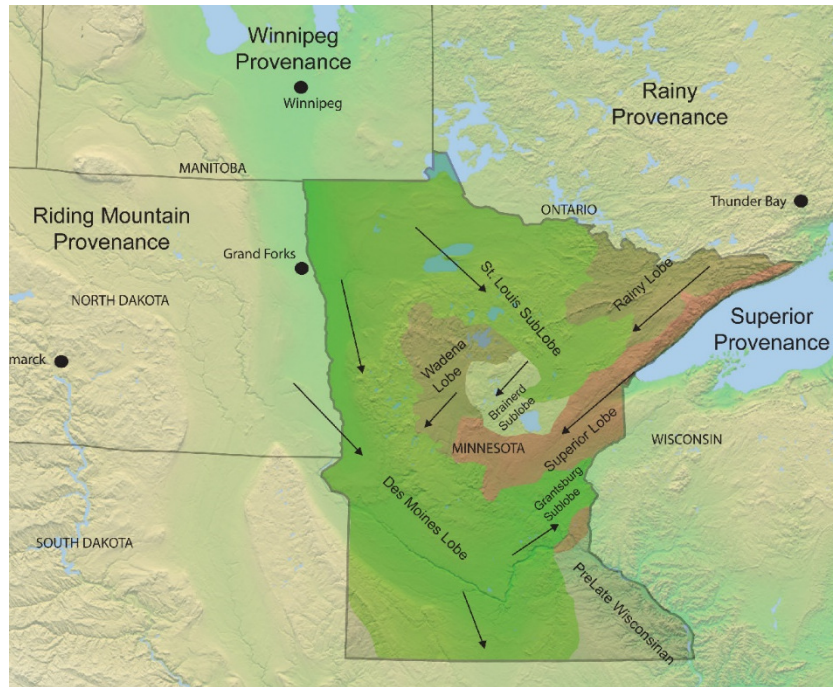


Figure 1. Map of Wisconsin Age glacial movement in Minnesota (www.mngs.umn.edu)



Figure 2. Map displaying Renville County in Minnesota

Description of studied material

This study focused on a core (RNR-2) collected from Renville County, MN (Figure 2) by the Minnesota Geological Survey (MGS). MGS observed six till units within the core. The units, from top to bottom in the core, are as follows: Heiberg Member, Villard Member, Traverse des Sioux Formation, Good Thunder 1, Good Thunder 2, and Good Thunder 3. A simplified stratigraphic sequence of the core is shown in Figure 3. The Heiberg Member is within the New Ulm Formation and was deposited about 13,000 years ago during the late Wisconsin glaciation (Johnson et al. 2016). It is a pebbly to clayey loam diamicton and is light brown to gray in color (Johnson et al. 2016). The top 17 feet of the Heiberg Member in the RNR-2 core is oxidized (Knaeble, personal communication). The Villard Member is an older part of the New Ulm Formation and is a pebbly to clay loam diamicton, yellowish brown to gray brown in color (Johnson et al. 2016). The New Ulm Formation was deposited by the Des Moines Lobe after it travelled across North Dakota and the Red River

Valley, depositing till attributed to the Riding Mountain provenance (Johnson et al. 2016). The Villard Member contains less Cretaceous shale than the overlying layers, and may have a partial Winnipeg provenance (Johnson et al. 2016). The Traverse des Sioux Formation is a tan, sandy loam diamicton that lacks Cretaceous shale in many locations. Bedded silt and clay layers, indicating varved lake sediment, also occur within this unit (Johnson et al. 2016). The Traverse des Sioux has a mixed Rainy and Winnipeg provenance (Johnson et al. 2016). Good Thunder 1, 2 and 3 are

members of the larger Good Thunder Formation. All contain dark, fossiliferous limestone, but Good Thunder 3 also contains gray shale (Lusardi 2016). Good Thunder 1 and 2 are similar in appearance, and the presence of Good Thunder 2 within RNR-2 has been disputed (Knaeble, personal communication). The Good Thunder Formation is a pre-Illinoian glacial deposit and is composed of 4, possibly 5, carbonate-rich diamicton units (Johnson et al. 2016). The formation is thought to have a north-northwest source based on the abundance of Paleozoic carbonate clasts (Johnson et al. 2016).

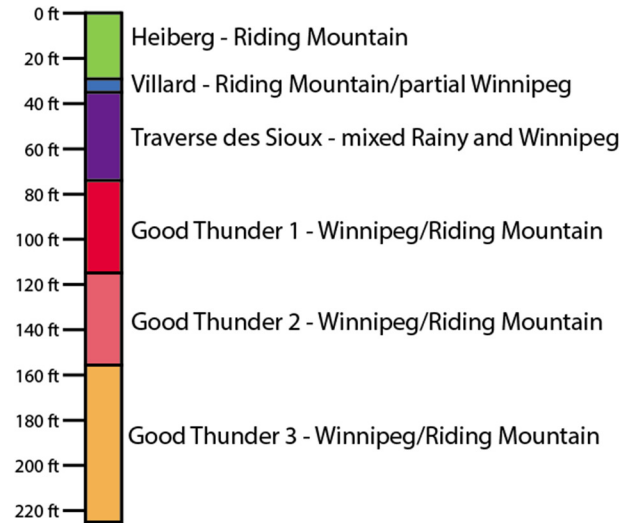


Figure 3. Simplified stratigraphic sequence for the analyzed core from Renville County, MN (RNR-2).

METHODS

Till samples of 100 g were received from the Minnesota Geological Survey (MGS), who collected them every 4 to 5 ft from individual units in the Renville County core (RNR-2). The less than 2 mm (<2) size fraction for each sample was separated by dry sieving, and subsamples of this size fraction were reserved for analysis. The remaining <2 fraction was sieved again to obtain a less than 63 μm (<63) size fraction. A subsample of the <63 fraction was also reserved. Each subsample contained enough material so that approximately 1 g of sediment would remain after carbonate removal, based on percent carbonate values provided by MGS (Knaeble, personal communication).

Carbonates from each sample were removed using a pH 5.0 acetic acid buffer solution. The samples with buffer solution were placed in a 90°C hot water bath for 2 hours and left to settle overnight. After removal of the supernatant, the samples were rinsed with DI water. Each sample was then dried overnight in a 100°C oven. After drying, lithium metaborate fusion was used to prepare for ICP-MS analysis.

The sieved samples were homogenized in a ball mill. Rock powder (0.15 g) of each sample and lithium metaborate (0.75 g) were added to a graphite crucible. The crucibles were placed in a furnace at 1000°C for 10 minutes with subsequent dissolution in 1 M nitric acid. 50-fold dilution of the initial solution and addition of an internal standard containing Be, Bi, In, Sc, Tb, and Ga to each sample occurred before ICP-MS analysis. In addition to the till samples, a sediment standard (Green River Shale, SGR-1) and 5 sample duplicates were also analyzed. The sediment standard was analyzed with and without carbonate. One duplicate came from each studied till member and both size fractions (3 from <63 and 2 from <2). The samples were analyzed on an Agilent 7700 Series ICP-MS for Ce, Dy, Er, Eu, Gd, Ho, La, Lu, Nd, Pr, Sm, Tm, U, Y, Yb, Sr, Mn, Rb, Ba, Zn, Pb, V, Cu, Cr, and Mo (25 elements in total).

Due to disparity in the stratigraphic interpretation involving Good Thunder 1 and Good Thunder 2, they were combined to represent one unit in statistical analysis (called Good Thunder C from here on out). All statistical analyses were completed for both size fractions. Two-way ANOVA tests were used to investigate the significance of the differences between till members for each measured element. A two-way ANOVA tests whether one group mean is significantly different from at least one other group mean. Principal component analysis (PCA) was used to assess the separation between till members using multiple elements. Samples within the Villard

member were removed from the multivariate analysis due to a small number of samples (n=2 for each size fraction). In a PCA, each element is an axis, and the data are plotted along these axes. The PCA model then assigns loadings to each variable to define an axis that best explains the variability in the data. It does this for every variable and rigidly rotates the data to fit on the plane formed by the two axes that explain the most variability. Discriminant function analysis (DFA) was performed to assess the predictive capability of the geochemical data. The elements included in the DFA were determined based on collinearity with other elements ($r > 0.85$) and the scaling factors from larger DFAs (elements with low scaling factors were removed). Cross validation for each sample was performed with the DFA by removing one sample, calculating the DFA and reinserting the sample to test whether it was placed in the correct group.

RESULTS

Individual element trends across units

Of the 25 elements analyzed, two (Lu and Mo) were removed from analysis because the measured concentrations in the samples were below detection limits. For the most part, the concentrations of trace elements in the <63 μm size fraction are higher and encompass a wider range than those for the <2 mm fraction (Figure 4). Additionally, visual trends among the units are observed. The upper members (Heiberg, Villard, and Traverse des Sioux) typically have higher concentrations of most elements than the Good Thunder members. When this is not the case, all of the members have roughly the same concentration (see Cu and U, Figure 4). Good Thunder C consistently has lower concentrations than the other units.

The relationship of rare earth elements among the different members was investigated using spider diagrams (Figure 5). Typically, rare earth elements have similar chemical behaviors, and spider diagrams are used to analyze trends across the suite of elements compared to a reference standard. Post-Archean Australian Shale (PAAS) was used as the reference material when constructing the spider diagrams. Concentrations for each element were averaged for each member and are separated by size fraction. The <2 mm fraction is the top diagram in Figure 5. The lines in this diagram are uniform, and do not exhibit separation between the members. The Villard and Good Thunder C members have different trends for thulium than the other three and are inverses of each other. The <63 μm fraction (bottom diagram in Figure 5), however, does show separation between the till members, but the overall trends from element to element remain consistent. Good Thunder C has concentrations that are visibly lower than the others. Good Thunder 3 also has a lower concentration than the other units, but the difference is not as drastic as in Good Thunder C.

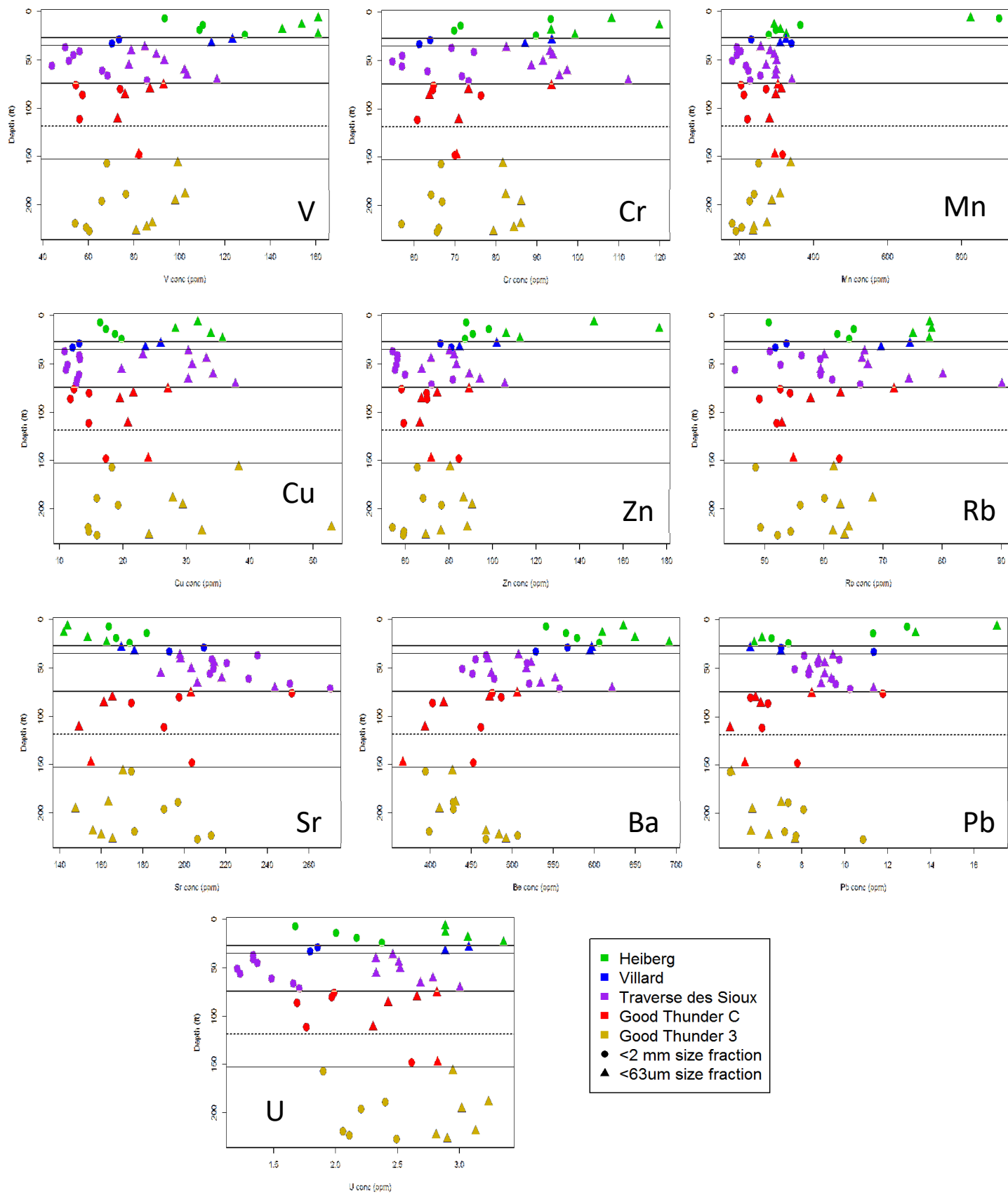


Figure 4. Stratigraphic patterns of concentration (ppm) for the analyzed trace elements. The colors correspond to the various till members, and both size fractions are presented. Solid horizontal lines coincide with contacts between till members. The dashed horizontal line represents the transition from Good Thunder 1 and Good Thunder 2, which were combined in this analysis.

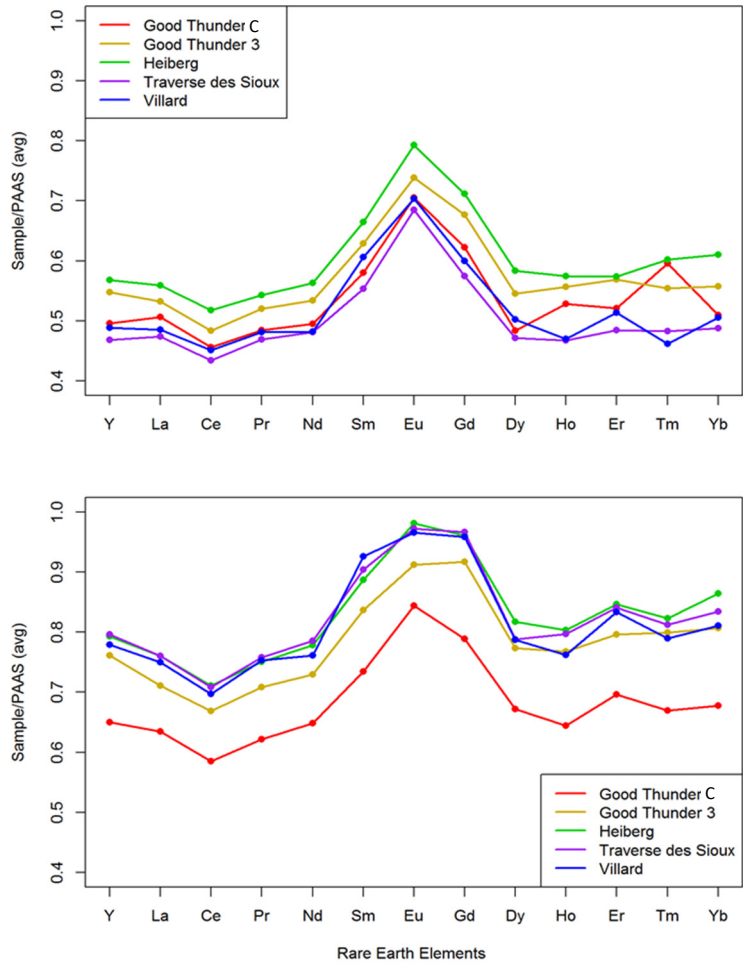


Figure 5. Spider diagrams of average concentration (normalized with PAAS) for each unit, separated by size fraction (<2 mm top, <63 μm bottom). PAAS = Post-Archean Australian Shale

Two-way ANOVA tests were used to assess which till members are significantly different from the other members for each of the individual elements. Table 1 outlines the significance of each element for the two size fractions at a 0.05 significance level.

Table 1. Results of the ANOVA tests of each element for the two size fractions ($\alpha=0.05$). Trace elements on the left and rare earth elements on the right.

Element	Significant for <2 mm	Significant for <63 μm
Vanadium	Yes	Yes
Chromium	Yes	Yes
Manganese	Yes	No
Copper	Yes	No
Zinc	Yes	Yes
Rubidium	No	Yes
Strontium	Yes	Yes
Barium	Yes	Yes
Lead	No	Yes
Uranium	Yes	Yes

Element	Significant for <2 mm	Significant for <63 μm
Yttrium	No	Yes
Lanthanum	No	Yes
Cesium	No	Yes
Praseodymium	No	Yes
Neodymium	No	Yes
Samarium	No	Yes
Europium	No	Yes
Gadolinium	No	Yes
Dysprosium	No	Yes
Holmium	No	Yes
Erbium	No	Yes
Thulium	No	Yes
Ytterbium	No	Yes

The trends between trace and rare earth elements are drastically different. In the trace elements (left in Table 1), at least one of the till unit concentrations was significantly different from the others in 8 of the 10 elements for both size fractions. In the rare earth elements, however, at least one of the till members was significantly different from the others for every element in the <63 μm fraction but for zero of them in the <2 mm fraction. This finding can also be seen in the spider diagrams in Figure 5.

Multivariate analysis

While the ANOVA tests indicated that significant differences exist in the geochemistry of the units, the differences often occurred between groups of units. For example, the vanadium concentration of the Heiberg member in the <2 mm fraction was significantly higher than the other four, but the other four were not significantly different from each other. Principal component analysis (PCA) was used to investigate differences among the units based on the relationships among elements. The biplots for each size fraction are displayed in Figures 6 (<2 mm) and 7 (<63 μm). For the multivariate analyses, Villard samples were removed because the small sample size ($n=2$) would not provide sufficient predictive power.

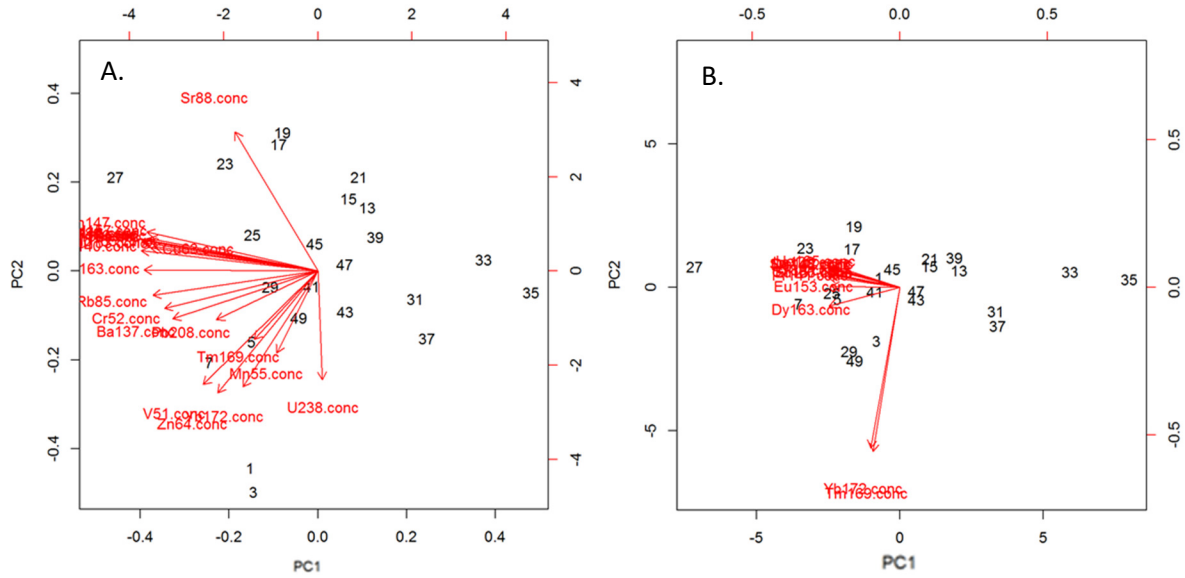


Figure 6. PCA results for the <2 mm fraction; all analyzed elements on the left and rare earth elements only on the right. The arrows in the plots indicate loadings.

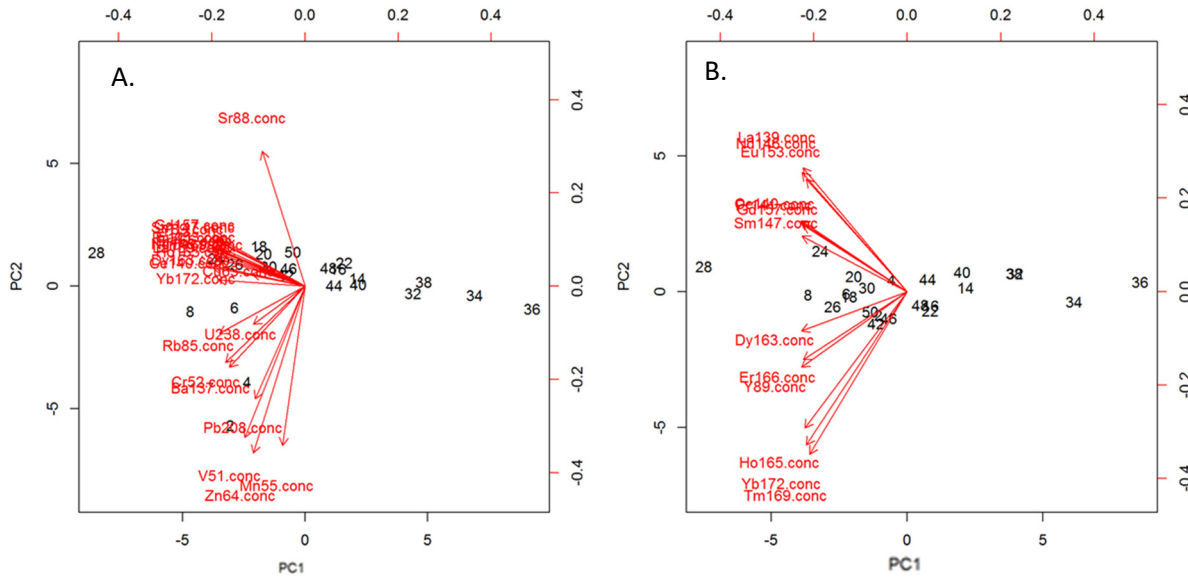


Figure 7. PCA results for the <63 μm fraction; all analyzed elements on the left and rare earth elements only on the right. The arrows in the plots indicate loadings.

PC1 and PC2 are the principal components (combinations of variables) that describe the most variability in the data; in both size fractions, over 90% of the variability was captured by PC1 and PC2 together. The orientation and length of the arrows in the biplots indicate the magnitude of loading for each principal component. For the <2 mm fraction, PC1 depends

mostly on the rare earth elements (the mass of red in Figure 6), while PC2 depends primarily on Sr, Mn, Zn, Cu, Cr, Ba, and V. The <63 μm PC1, similar to the < 2 mm fraction, primarily depends on the rare earth elements, and PC2 depends on Sr, Mn, V, Zn, and Pb.

In both size fractions, the rare earth element arrows plot almost exactly on top of one another. Matching arrow in the biplots indicate possible multicollinearity in the variables and was confirmed using a correlation matrix. A PCA was done using only the rare earth elements to determine whether groups of rare earth elements exhibited different trends (Figures 6B and 7B). The rare earth elements plotted in two groups for the <2 mm fraction and in four groups for <63 μm . When trying to distinguish among units, multicollinearity causes many problems because the similar elements will not provide additional information and at worst, cause misclassifications due to one anomalous element. A preliminary discriminant function analysis (DFA) was completed using all elements to identify the most influential using the determined scaling factor (Table 2). Elements included in the final DFA were determined in the following way:

1. Element was checked for multicollinearity using the PCA and correlation matrix.
2. The collinear element with the highest scaling factor was included.
3. If an element was not collinear with any other, but had a low scaling factor (absolute value <0.01), it was removed and the cross-validation matrices of the two DFAs were compared. This is explained below.

Due primarily to the difference in multicollinearity between the rare earth elements in the size fractions, the number of elements included in the DFAs for each size fraction differ (Figures 5-8).

Table 2. Scaling factors of the initial DFA. * = element collinear with at least one other element in <2 mm fraction. + = element collinear with at least one other element in <63 μm fraction ($r > 0.85$).

Element	LD1 Scaling (<2 mm)	LD2 Scaling (<2 mm)	LD1 Scaling (<63 μm)	LD2 Scaling (<63 μm)
Vanadium*+	0.4007	0.2141	1.0678	-0.1527
Chromium*+	-0.0381	-0.0892	-0.2392	0.0761
Manganese	0.0040	-0.0155	-0.0331	0.0124
Copper	0.1222	0.0190	0.2894	-0.1929
Zinc*+	0.0549	-0.1019	-0.0784	0.0612
Rubidium*+	-0.3651	-0.1882	-0.6686	-0.1440
Strontium	-0.0805	0.0336	-0.0148	0.0547
Barium*+	0.0678	0.0015	-0.0049	0.0363
Yttrium*+	-1.3738	0.6733	-2.5775	-0.7511
Lanthanum*+	1.0648	0.3450	-4.3479	-0.5164
Cesium*+	-2.1279	-0.5620	-3.2468	-0.0460
Praseodymium*+	-5.8922	-1.0768	22.9598	3.9900
Neodymium*+	0.6049	0.5790	4.6471	-1.1218
Samarium*+	11.1151	-1.3826	8.2533	3.5860
Europium*+	-8.2911	8.0327	14.7217	2.4753
Gadolinium*+	3.1219	3.3561	-11.2379	-5.4353
Dysprosium*+	3.4402	0.1862	-0.5301	4.4278
Holmium*+	43.7243	10.2828	26.9168	-6.8708
Erbium*+	-10.2917	-2.5510	10.3790	-4.4379
Thulium+	10.2654	-50.1428	45.6732	14.3787
Ytterbium+	7.9731	9.4368	-3.5877	-7.2135
Lead	-0.1725	1.5705	1.4631	-0.3293
Uranium	0.3007	-11.4072	-10.6904	18.7158

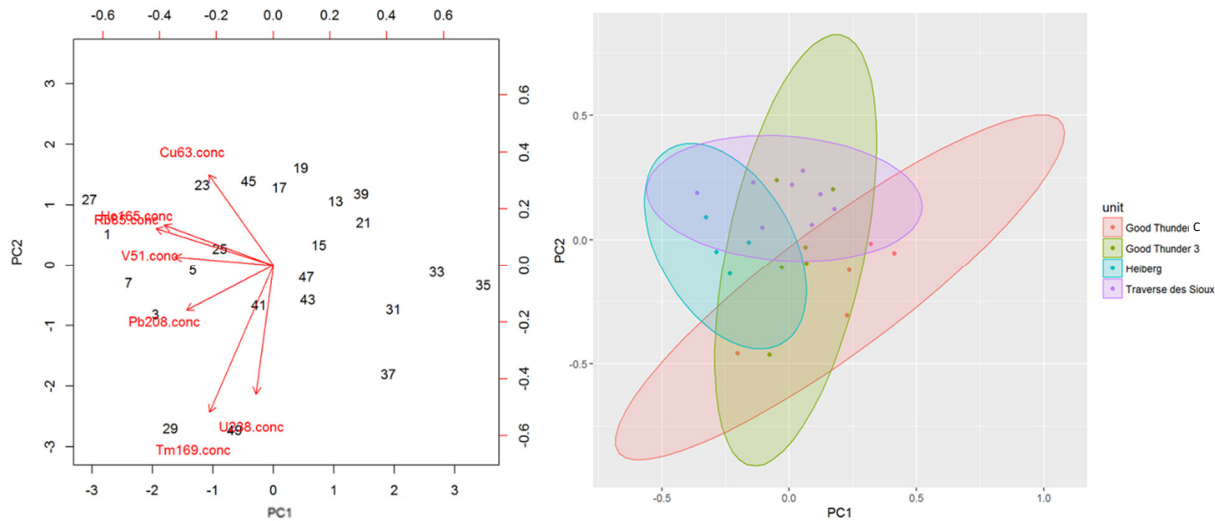


Figure 8. PCA results of elements included in the final DFA model for the <2 mm fraction. Biplot on the left and 95% probability ellipses on the right. Different relationships among the elements are seen by the different orientations of the probability ellipses.

Element	LD1 Scaling	LD2 Scaling
Vanadium	0.2027	-0.0076
Copper	0.0149	0.0551
Rubidium	-0.2592	-0.0497
Holmium	-1.9372	-13.9298
Thulium	11.1184	10.3256
Lead	0.00618	-0.0129
Uranium	-0.4621	3.0125

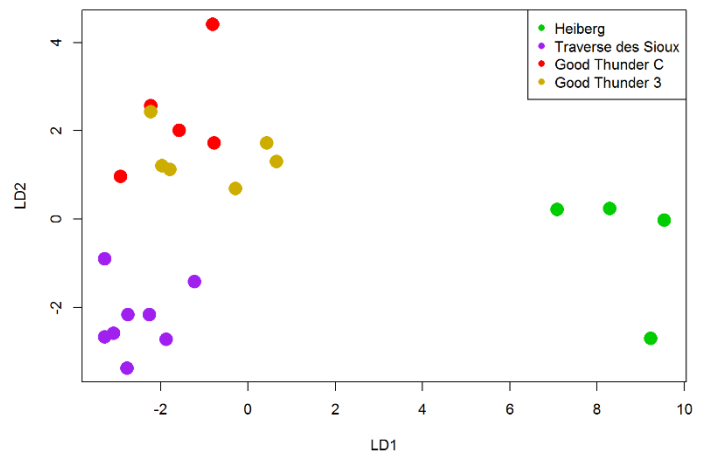


Figure 9. Results of final DFA for the <2 mm fraction. Table of scaling factors on the left and plot of unit groupings on the right. In the plot on the right, the samples are approximately separated by unit, with some overlap between Good Thunder C and Good Thunder 3.

Seven elements were used to construct the DFA for the <2 mm fraction. Copper and lead have low scaling factors, but each is the sole element used to identify specific trends in the variability (see biplot in Figure 8). For perfect separation, the ellipses in Figure 8 would not overlap. However, the differences in long axis direction indicates different relationships among elements. These differences can be used to distinguish among units. The samples are approximately grouped according to unit in the plot in Figure 9, indicating high predictive power

of the model. Removal of additional elements led to a lower cross-validation percentage (see Cross-validation section below). The most influential element by scaling factor was thulium (Table 2).

Ten elements were needed for the <63 μm fraction (Figure 11). Copper and chromium had the lowest scaling factors, but each is associated with a certain relationship. The copper relationship looks similar to uranium in the biplot in Figure 10, but the cross-validation percentage fell considerably when copper was removed. The ellipses in Figure 10 overlap, but again most have different orientations. Good Thunder C and Traverse des Sioux have approximately the same orientation so the predictive power between these units may be lower than in the <2 mm fraction. Somewhat surprisingly, the samples are again mostly separated according to unit in Figure 11. There is much more overlap between Good Thunder C and Good Thunder 3 in the DFA for <63 μm than in the <2 mm DFA. The most influential element for the <63 μm fraction is thulium, which is the same as the <2 mm fraction.

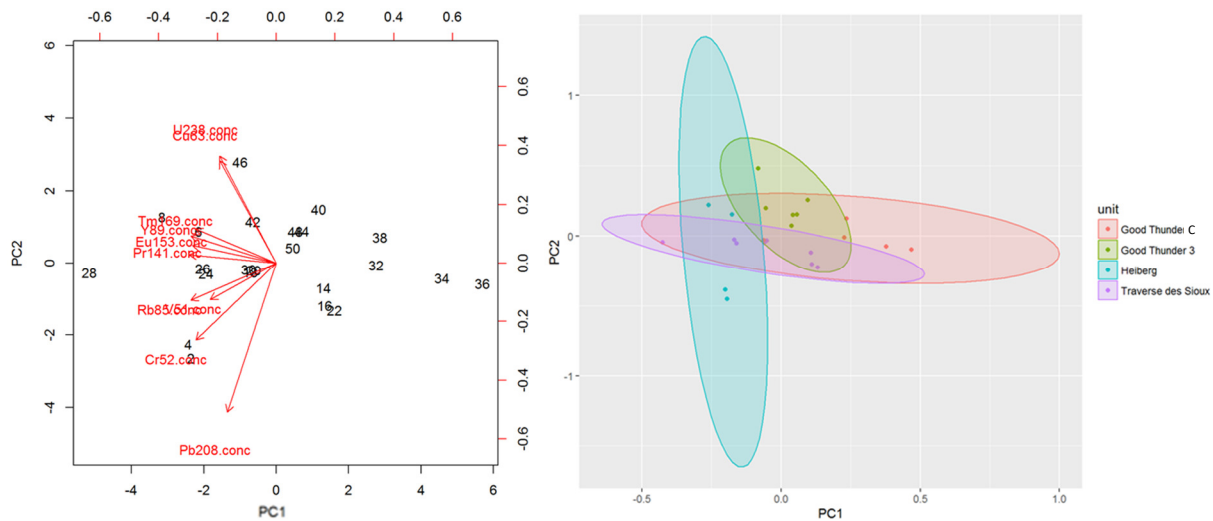


Figure 10. PCA results of elements included in the final DFA model for the <63 μm fraction. Biplot on the left and 95% probability ellipses on the right. Different relationships among the elements are seen by the different orientations of the probability ellipses.

Element	LD1 Scaling	LD2 Scaling
Vanadium	0.2268	0.0048
Chromium	0.0198	0.0211
Copper	0.0426	-0.0736
Rubidium	-0.2096	-0.0028
Yttrium	1.3844	-1.2601
Praseodymium	0.1068	-2.2491
Europium	-5.3735	1.7278
Thulium	-27.8426	39.2465
Lead	-0.1108	0.0357
Uranium	-8.3839	10.4363

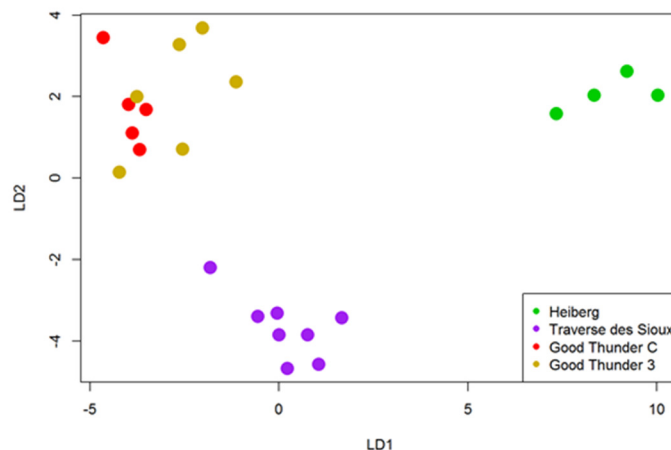


Figure 11. Results of final DFA for the <63 μm fraction. Table of scaling factors on the left and plot of unit groupings on the right. In the plot on the right, the samples are approximately separated by unit, with considerable overlap between Good Thunder C and Good Thunder 3.

Cross-validation

Cross-validation is a good way to test a model in the absence of a test dataset. One sample is removed from the data, a model is created without the sample, and then the sample is classified according to this model. The model classification is compared with the correct classification. This is repeated for every sample in the data set.

Cross-validation was performed on both DFAs (results in Tables 3 and 4). Perfect classification corresponds to values only appearing on the diagonal of the cross-validation matrix. The percent of samples correctly classified by the model is found by dividing the sum of the values on the diagonal by the total number of samples. The <2 mm DFA correctly classified 86.9% of the samples and the <63 μm classified 82.6% correctly.

Table 3. Cross-validation table for the <2 mm DFA. Rows represent the correct classification, and columns denote the model determination. The upper left corner gives the percent of samples correctly classified.

86.9%	Good Thunder C	Good Thunder 3	Heiberg	Traverse des Sioux
Good Thunder C	3	1	0	1
Good Thunder 3	1	5	0	0
Heiberg	0	0	4	0
Traverse des Sioux	0	0	0	8

Table 4. Cross-validation table for the <63 µm DFA. Rows represent the correct classification, and columns denote the model determination. The upper left corner gives the percent of samples correctly classified.

82.6%	Good Thunder C	Good Thunder 3	Heiberg	Traverse des Sioux
Good Thunder C	4	1	0	0
Good Thunder 3	1	4	0	1
Heiberg	0	0	4	0
Traverse des Sioux	0	1	0	7

Checking Villard samples

The Villard samples were removed from model creation because of the low number of samples. The DFA was run to include their data, to see where they plot (Figure 12). In both models, the Villard samples plot in a region of their own, so the potential exists to include Villard in the model given more data.

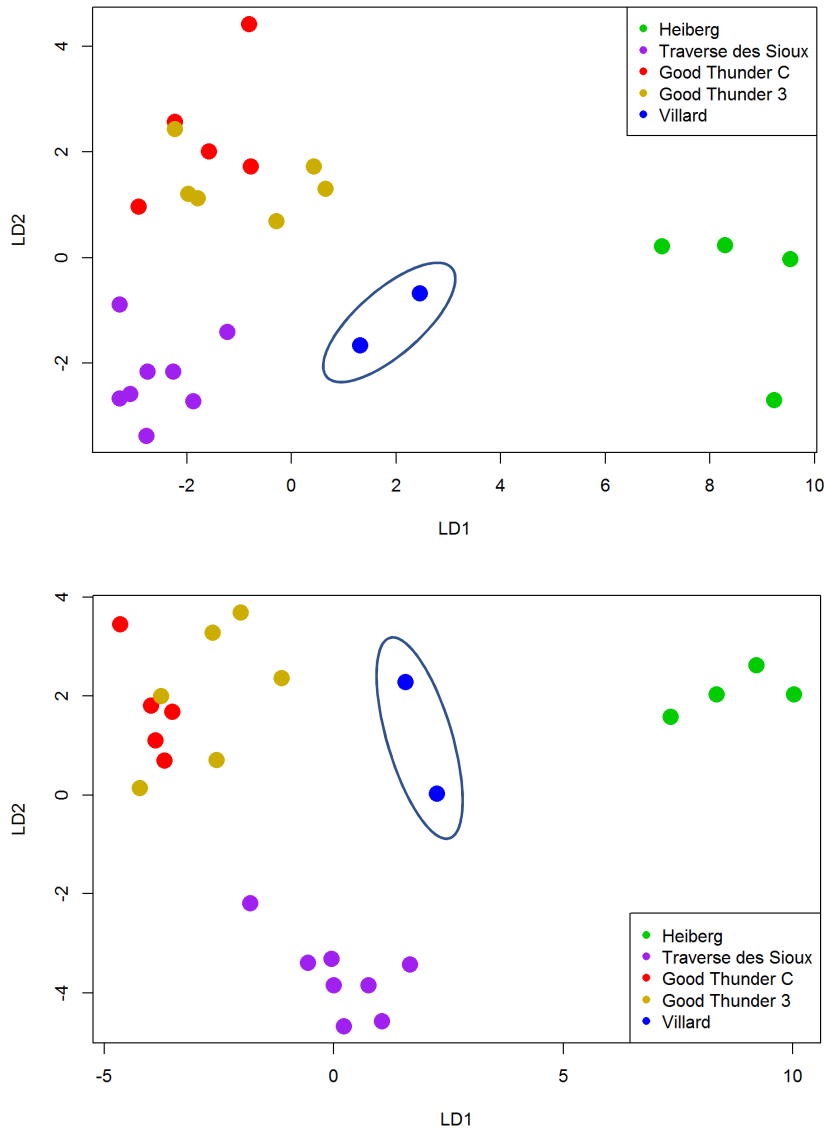


Figure 12. Plots of unit groupings for the two DFAs. Villard samples are overlain (blue). Top: <2 mm and Bottom: <63 μm .

DISCUSSION

Minnesota has four general provenance areas, with multiple glacial advances originating from each area. Rainy provenance deposits typically are brown, sandy tills with basalt and gabbro (Gowan 1998). Winnipeg provenance tills are gray and are limestone-bearing (Thorleifson 2007). Superior provenance tills are redder in color and contain sandstones, shales, and agates (Gowan 1988). Riding Mountain provenance deposits, typically Des Moines Lobe tills, are gray to brown and have abundant Cretaceous shale (Lively 2009). The differences among tills of different provenance can be difficult to discern through clast counts as limestones and less stable minerals weather. Because these differences are due to differences in mineralogy, and mineralogy controls the chemistry of the till, geochemical patterns may provide a robust tool to determine provenance.

Trace and rare earth elements, along with multivariate statistical analysis, can be used to distinguish among till members. Multivariate analysis is required because any single element does not partition such that each till can be identified from the concentration of an individual element. Comparing the trends in Figures 4 and 5 also highlight this observation, as at least two members encompass a similar range of concentrations for each element. The rare earth elements (Figure 5) show separation between the members even though the units have similar trends across the elements. Because each member has a similar trend, the rare earth elements could be consolidated into a smaller number within the multivariate analysis without losing analytic power.

This is also valid geochemically, as rare earth elements exhibit similar behavior during mineral formation and weathering. Europium is typically enriched and cesium is depleted in shales (Ohlander 1996); the spider diagrams in Figure 5 display this behavior for every member, and confirm the textural observations made by MGS (Knaeble, personal communication). One of the most striking results from this investigation is the number of rare earth elements included in the discriminant function analysis (DFA) for each size fraction. Two rare earth elements (holmium and tellurium) were included in the model for the <2 mm size fraction, but four (yttrium, praseodymium, europium, and tellurium) were used in the model for the <63 μm fraction. This seems to contradict the findings from the individual ANOVAs presented in Table 1. At least one member was significantly different from the others for each rare earth element in the <63 μm fraction, and none were for the <2 mm fraction. The spider diagrams (Figure 5),

however, highlight what may be causing this discrepancy. Rare earth elements tend to be associated with the clay fraction, so naturally their concentrations are higher in the < 63 μm fraction (Shilts 1995). This is observed in Figure 5, but the scaling for each element is not consistent between the size fractions. The units with large amounts of shale – Heiberg and Villard – exhibit higher concentrations than the carbonate richer Good Thunder units, effectively separating the units. This phenomenon also magnified the differences in concentration between the units, and may have identified underlying relationships that could not be observed in the <2 mm fraction due to dilution with chemically homogeneous sand grains.

The biplots for the principal component analysis in Figures 6 and 7 (right side) suggest that the rare earth elements do not behave similarly as a whole, but that groups of them behave similarly. The rare earth elements are separated into two groups in the <2 mm size fraction and into four groups in the <63 μm fraction. The chemical explanation for this is beyond the scope of this project, but this difference is highlighted because it may influence which size fraction is best to measure for distinction of till units.

Within the trace elements, there were also elements that correlated well with one another or did not have a significant influence on the model. Those that correlated well with another (Zn with Cr and V, Ba with Rb) were removed from the model – the one with the highest scaling from higher order models was chosen – because they did not provide additional information. Additionally, the elements with very low scaling factors in the model (Sr, Mn) were also removed. Strontium is typically associated with carbonates (Shilts 1995); because the carbonates were removed prior to analysis, it is reasonable that the strontium concentration between the units was not as influential as another element. The geochemical reason for why these elements either correlated with each other or barely influenced the model is beyond the scope of this investigation.

The total number of elements included in the DFA models (see Figures 9 and 11) differed between the two size fractions. The model for the <2 mm size fraction included 7 elements (see Figure 9) while the one for <63 μm has 10 elements (Figure 11). The main difference between the two models is both the number and identity of the rare earth elements, as discussed earlier. The model for the <2 mm fraction had a slightly higher cross validation accuracy (approximately 87% for <2 mm and 83% for <63 μm). This separation is observed in Figures 9 and 11 as each unit is mostly separated from the others. Neither model fully distinguished between the two

Good Thunder units, but the <2 mm model shows slightly more separation between them. These units have the same provenance, and the textural distinction was made based on the abundance of clay in each (Knaeble, personal communication), so their geochemical signatures are expected to be more similar than the other investigated units. The cross validation also suggests that there is some basal mixing within stratigraphically adjacent units. Tables 3 and 4 contain the assignments during cross validation. Within the model for <2 mm, all the misclassifications occurred between adjacent units that MGS identified as having some basal mixing (Knaeble, personal communication). There were more misclassifications in the <63 μm model, and some of the misclassifications were between the Traverse des Sioux and Good Thunder 3. These units have a partial shared provenance, so the misclassification is acceptable, but they are not adjacent units, indicating the <63 μm model has more trouble distinguishing between the units than the <2 mm model.

The positions of the till units in the DFA (Figure 12) correspond well with their provenance relationships. The far right of the DFA plot (positive on LD1) corresponds with Riding Mountain provenance. The Heiberg unit is unmixed Des Moines Lobe till, so it plots with a large positive value on LD1. Riding Mountain tills contain large proportions of shale, which metals like vanadium, chromium, and rare earth elements tend to adsorb to. This drives the LD1 values for Heiberg far to the right. The far left (negative or near zero on LD1) corresponds to mostly Winnipeg provenance, which was represented by the Good Thunder units. Winnipeg tills contain large proportions of carbonate, which has been associated with elevated lead concentrations. Even though the carbonates were removed, the lead ions in solution could adsorb to the clay particles after dissolution. The Traverse des Sioux was the only studied till containing partial Rainy provenance, and was the only unit to plot negative on LD2. This was driven by high rubidium concentrations, and its magnification in the <63 μm fraction indicates that rubidium is mostly found in the fine size fraction. The extent of Rainy provenance tills on the DFA plot is likely more negative along LD2 because rubidium-rich feldspars have been found in pegmatite within the Winnipeg provenance area (Cerny 1972). Further confirmation of the proposed extent on the DFA plots is the location of the Villard unit, which plots almost exactly between the Heiberg and the Good Thunder units. The Villard is a majority Riding Mountain, partial Winnipeg provenance so it should plot between the Good Thunder and Heiberg units using the proposed zones.

One aspect of the DFA that must be considered are the statistical assumptions. The Villard member was not included in the model and the Good Thunder 1 and 2 units were combined because of small sample size. Even with these measures, the sample sizes for each till unit were small for DFA. This investigation, however, tested whether trace and rare earth elements can be used to distinguish among till members. The results indicate that it is indeed possible, and a data analysis technique was also developed. The analysis revolves around using principal component analysis as an exploratory analysis to identify potential elements of interest, and then to develop a predictive model using DFA. A benefit of using DFA is that it can be continuously updated as more data is collected.

Even with the small sample size, the proposed analysis technique successfully differentiated among four Minnesota till members with north to northwest provenances, and possibly could have with another had the sample size been larger. This type of analysis would work best within a hierarchy of till analysis schemes. This hierarchy can begin with clast counting and textural analysis, then move to x-ray diffraction and major element geochemistry, and then move to the trace and rare earth element analysis used in this investigation. The DFA used in this study can be improved and made more comprehensive by including data on more types of till and for different provenances – including tills with a Superior provenance would be a great first step. Additionally, the models developed in this investigation are specific to the Heiberg, Traverse des Sioux, the combined Good Thunder 1 and 2, and Good Thunder 3. With more data on the Villard and Good Thunder 2, the analysis could also be used to differentiate between these as well, based on the concentration patterns with depth in Figure 4.

Some of the steps in sample preparation and measurement can also be further investigated. Carbonates were removed because the primary geochemical information is thought to be contained in the clastic fraction (Shilts 1995). Repeating this investigation without removing the carbonates may prove beneficial, especially in developing a statewide geochemical survey as time and money can be saved by skipping the carbonate dissolution steps. Additionally, the geochemistry of tills may change spatially, as tills further from the source may be more weathered than those closer to the source. Investigations into the spatial relationship may indicate that developing models for different areas throughout Minnesota is best. The analysis technique presented in this study will still work under these circumstances, and can be updated accordingly for best results.

CONCLUSION

This thesis demonstrated that geochemical fingerprinting, combined with multivariate analysis, is a viable method to determine till provenance. Additionally, it was determined that using the <2 mm size fraction in analysis is sufficient, even though the measured concentrations of elements was less than in the <63 μm fraction. The geochemical patterns can be explained according to the mineralogy of the tills. Tills with large proportions of shales (Riding Mountain provenance) plot in a drastically different region of the two-dimensional space defined by a discriminant function analysis than tills with large proportions of carbonates (Winnipeg provenance). This was explained by the propensity of rare earth elements to adsorb to clay sized particles.

REFERENCES

- Cerny, P., and Macek, J., 1972, The Tanco Pegmatite at Bernic Lake, Manitoba: *Canadian Mineralogist*, v. 11, p. 679-689.
- Dempster, M., Dunlop, P., Scheib, A., and Cooper, M., 2013, Principal component analysis of the geochemistry of soil developed on till in Northern Ireland: *Journal of Maps*, v. 9, no. 3, p. 373-389.
- Erickson, M. L., and Barnes, R. J., 2005, Glacial sediment causing regional-scale elevated arsenic in drinking water: *Ground Water*, v. 43, no. 6, p. 796-805.
- Farmer, G. L., Licht, K., Swope, R. J., and Andrews, J., 2006, Isotopic constraints on the provenance of fine-grained sediment in LGM tills from the Ross Embayment, Antarctica: *Earth and Planetary Science Letters*, v. 249, no. 1-2, p. 90-107.
- Gore, D. B., Snape, I., and Leishman, M. R., 2003, Glacial sediment provenance, dispersal and deposition, Vestfold Hills, East Antarctica: *Antarctic Science*, v. 15, no. 2, p. 259-269.
- Gowan, A. S., 1998, *Methods of till analysis for correlation and provenance studies in Minnesota*: Minnesota Geological Survey: St. Paul, MN, United States, 00769177.
- Grasby, S. E., Osborn, J., Chen, Z., and Wozniak, P. R. J., 2010, Influence of till provenance on regional ground water geochemistry: *Chemical Geology*, v. 273, no. 3-4, p. 225-237.
- Hobbs, H.C, 1998, *Use of 1-2 millimeter sand-grain composition in Minnesota Quaternary studies*: Minnesota Geological Survey: St. Paul, MN, United States, Report of Investigations 49, p 193-208.

- Johnson, M. D., Adams, R. S., Gowan, A. S., Harris, K. L., Hobbs, H. C., Jennings, C. E., Knaeble, A. R., and Lusardi B. A., Meyer, G. N., 2016, Quarternary lithostratigraphic units of Minnesota: Minnesota Geological Survey: St. Paul, MN, United States, 0076-9177.
- Klassen, R. A., 1998, Geological factors affecting the distribution of trace metals in glacial sediments of central Newfoundland: *Environmental Geology*, v. 33, no. 2-3, p. 154-169.
- Klassen, R.A., 2001, A Quaternary geological perspective on geochemical exploration in glaciated terrain: *Drift Exploration in Glaciated Terrain*, v. 185, p. 1-17.
- Lively, R. S., and Thorleifson, L. H., 2009, Minnesota soil, till, and ground-water geochemical data: Minnesota Geological Survey: St. Paul, MN, United States, OFR-09-02.
- Lunkka, J. P., Peuraniemi, V., and Nikarmaa, T., 2013, Application of till geochemical and indicator mineral data to the interpretation of the thick till sequence at Muhos, northern Finland: *Geochemistry-Exploration Environment Analysis*, v. 13, no. 3, p. 183-193.
- McMartin, I., Dredge, L.A., Grunsky, E., and Pehrsson, S., 2016, Till Geochemistry in West-Central Manitoba: Interpretation of Provenance and Mineralization Based on Glacial History and Multivariate Data Analysis: *Economic Geology*, v. 111, p. 1001-1020.
- Ohlander, B., Land, M., Ingri, J., and Widerlund, A., 1996, Mobility of rare earth elements during weathering of till in northern Sweden: *Applied Geochemistry*, v. 11, p. 93-99.
- Shilts, W. W., 1995, Geochemical partitioning in till: Ministry of Energy, Mines and Petroleum Resources: Victoria, Canada, 1995-2.
- Thorleifson, L. H., Harris, K. L., Hobbs, H. C., Jennings, C. E., Knaeble, A. R., Lively, R. S., Lusardi, B. A., and Meyer, G. N., 2007, Till geochemical and indicator mineral reconnaissance of Minnesota: Minnesota Geological Survey: St. Paul, MN, United States, OFR-07-01.

APPENDIX A

Quality Assurance and Quality Control

The detection limit corresponded to the concentration of the lowest calibration standard. The method blanks were comparable to the acid blanks, as three element concentrations (La, Cr, Ba) were significantly higher at a 0.05 significance level according to a t-test. All three of the concentrations in the method blanks were still considerably lower than the calibration standards, so they remained in the analysis.

Comparison of the Green River Shale (SGR-1) sediment standard to reported values by USGS (https://crustal.usgs.gov/geochemical_reference_standards/shale.html) shows that the fusion process did not influence concentrations of the studied elements. Measured chromium and zinc were above the reported values, and strontium and lead were below reported values. These elements are typically separated into the clastic and carbonate fractions, respectively, so the observed trend was likely due to a heterogeneous sample of the standard. The standard used may have had more clastic material and less carbonate than the parent standard. All the other elements fell within the reported ranges, so there was no suspicion of contamination through the method.

The sample duplicates also did not indicate any contamination through the method. 18 of the 23 analyzed elements were less than 10% different between duplicates. Lead had the highest average percent difference (34.73%). The other four elements (Cu, Zn, V, Cr) were less than 20% different on average. Copper and zinc were both higher than 15% different between duplicates, while vanadium and chromium had average differences between 10 and 15%.

APPENDIX B

Calibration Standards Used

Trace and Rare Earth Element Standards (TRRE-1 through TRRE-5)					
PPB	TRRE-1	TRRE-2	TRRE-3	TRRE-4	TRRE-5
Ce, Dy, Er, Eu, Gd, Ho, La, Lu, Nd, Pr, Sm, Tm, U, Y, Yb	50	10	1	0.1	0.01
Sr	6000	1000	500	50	10
Mn, Rb, Ba, Zn, Pb, V, Cu, Cr, Mo	600	100	50	5	1
ISTD (Be, Bi, In, Sc, Tb, Ga)	100	100	100	100	100

Post Archean Australian Shale (PAAS)

McLennan, S.M., 1989, Rare earth elements in sedimentary rocks: Influence of provenance and sedimentary processes

Table 2. REE abundances in various cosmochemical and geochemical reservoirs (ppm except where noted).

	Atom Abundance(Si=10 ⁶)		-----Sediments-----					Continental Crust ⁸		Igneous Rocks ⁹	
	Solar ¹	CI Chondrite ²	Chondrite ³	PAAS ⁴	NASC ⁵	ES ⁶	Loess ⁷	Upper	Total	Andesite	MORB
La	0.31	0.46	0.367	38.2	32	41.1	35.4	30	16	19	3.7
Ce	0.81	1.2	0.957	79.6	73	81.3	78.6	64	33	38	11.5
Pr	0.12	0.18	0.137	8.83	7.9	10.4	8.46	7.1	3.9	4.3	1.8
Nd	0.39	0.85	0.711	33.9	33	40.1	33.9	26	16	16	10.0
Sm	0.14	0.27	0.231	5.55	5.7	7.3	6.38	4.5	3.5	3.7	3.3
Eu	0.1	0.099	0.087	1.08	1.24	1.52	1.18	0.88	1.1	1.1	1.3
Gd	0.30	0.34	0.306	4.66	5.2	6.03	4.61	3.8	3.3	3.6	4.6
Tb	-	0.060	0.058	0.774	0.85	1.05	0.81	0.64	0.60	0.64	0.87
Dy	0.26	0.40	0.381	4.68	5.8	-	4.82	3.5	3.7	3.7	5.7
Ho	-	0.089	0.0851	0.991	1.04	1.20	1.01	0.80	0.78	0.82	1.3
Er	0.19	0.26	0.249	2.85	3.4	3.55	2.85	2.3	2.2	2.3	3.7
Tm	0.042	0.039	0.0356	0.405	0.50	0.56	-	0.33	0.32	0.32	0.54
Yb	0.2	0.25	0.248	2.82	3.1	3.29	2.71	2.2	2.2	2.2	3.7
Lu	0.13	0.038	0.0381	0.433	0.48	0.58	-	0.32	0.30	0.30	0.56
ΣREE			3.89	184.8	173	204	181	146	87	96	52.6
La _N /Yb _N			1.00	9.15	6.98	8.44	8.83	9.21	4.91	5.84	0.68
La _N /Sm _N			1.00	4.33	3.53	3.54	3.49	4.20	2.88	3.23	0.71
Eu/Eu*			1.00	0.65	0.70	0.70	0.66	0.65	0.99	0.92	1.02
Sc	28	34.5	8.64	16	14.9	-	8.4	11	30	30	38
Y	4.0	4.33	2.25	27	27	-	2.5	22	20	22	32

¹ - From Ross & Aller (1976); Aller (1987)

² - From Evensen et al. (1978); Schmitt et al. (1964)

³ - From Taylor & McLennan (1985). Note that Primitive Earth Mantle abundances (ie.- present mantle plus crust) are taken as 1.5 times these values.

⁴ - Average 23 post-Archean shales from Australia (adapted from Taylor & McLennan, 1985); see text for details

⁵ - Composite 40 shales, mainly N.American (Haskin et al., 1968; Gromet et al., 1984)

⁶ - Composite of numerous European shales (Haskin & Haskin, 1966)

⁷ - Carbonate-free loess (Taylor et al., 1983)

⁸ - From Taylor and McLennan (1985)

⁹ - Averages (Taylor & McLennan, 1985)



**United States Geological Survey
Certificate of Analysis**

Green River Shale, SGR-1

Sample for this reference material was collected from the Mahogany zone of the Green River Formation. It is a petroleum and carbonate-rich shale. At the time of preparation, shale oil tests yield 51 to 57 gallons per ton.

Element concentrations were determined by cooperating laboratories using a variety of analytical methods. Certificate values are based primarily on international data compilations (Abbey, 1983, Gladney and Roelandts, 1988, Govindaraju, 1994). Initial USGS studies (Flanagan, 1976) provide limited background information on this reference material.

Recommended values					
Oxide	Wt %	±	Oxide	Wt %	±
SiO ₂	28.2	0.21	CoO	8.38	0.17
Al ₂ O ₃	6.52	0.21	MgO	4.44	0.20
K ₂ O	1.66	0.10	P ₂ O ₅	0.328	0.066
Na ₂ O	2.99	0.13	TiO ₂	0.253	0.025
Fe ₂ O ₃ T	3.03	0.14	S _{tot}	1.53	0.11
Element	µg/g	±	Element	µg/g	±
As	67	5	Eu	0.56	0.09
B	54	3	F	1960	240
Ba	290	40	Hf	1.4	0.14
Ce	36	4	La	20	1.8
Co	12	1.5	Li	147	26
Cr	30	3	Mn	267	34
Cs	5.2	0.3	Mo	35	0.9
Cu	66	9	Nd	16	1.7
Er	1.1	0.14	Pb	38	4
Sb	3.4	0.5	Sc	4.6	0.7
Se	4.6	0.7	Sm	2.7	0.3
Si	2.7	0.3	Sr	420	30
Sr	420	30	Th	4.8	0.21
Th	4.8	0.21	U	5.4	0.4
U	5.4	0.4	V	130	6
V	130	6	W	2.6	0.06
W	2.6	0.06	Zn	74	9
Zn	74	9			
Oxide	Wt %		Oxide	Wt %	
Fe ₂ O ₃	1.46		FeO	1.41	
C _{tot}	28		Cinorg	3.2	
Element	µg/g		Element	µg/g	
Cd	0.9		Ho	0.4	
Cl	32		Li	147	
Dy	1.9		Nb	5.2	
Ga	12		Ni	29	
Gd	2		Se	3.5	
Hg	0.3		Sn	1.9	
			Tm	0.17	
			Y	13	
			Yb	0.94	
			Zr	53	

Denver, Colorado
revised May 2014

Dr. Stephen Wilson
Reference Material Project, CCGSC